Journal of Materials Chemistry A

Enhancement of catalytic hydrolysis activity for organophos-phates by the Metal-Organic Framework MOF-808-NH2 via post-synthetic modification.

Journal:	*Journal of Materials Chemistry A*
Manuscript ID	TA-ART-03-2023-001898.R1
Article Type:	Paper
Date Submitted by the Author:	18-May-2023
Complete List of Authors:	Garibay, Sergio; Leidos Inc; US Army Combat Capabilities Development Command Chemical Biological Center Tovar, Trenton; US Army Combat Capabilities Development Command Chemical Biological Center Iordanov, Ivan; DEVCOM, Peterson, Gregory; US Army Combat Capabilities Development Command Chemical Biological Center DeCoste, Jared; US Army Combat Capabilities Development Command Chemical Biological Center

SCHOLARONE™
Manuscripts

Enhancement of catalytic hydrolysis activity for organophosphates by the Metal-Organic Framework MOF-808-NH_2 via post-synthetic modification.

Sergio J. Garibay,[1,2] Trenton M. Tovar,[2] Ivan O. Iordanov,[2] Gregory W. Peterson,[2] and Jared B. DeCoste[2]*

[1]Leidos, Inc., 3465 Box Hill Corporate Center Drive, Abingdon, Maryland 21009, United States, USA.

[2]DEVCOM Chemical and Biological Center, 5183 Blackhawk Road, Aberdeen Proving Ground, Maryland 21010, USA.

ABSTRACT: Metal-organic frameworks (MOFs) necessitate buffers or basic amine moieties for high activity and turnover in the hydrolysis of organophosphates. While polymeric amine buffers can be integrated with a MOF, all solid-state formulations suffer from active site poisoning of the secondary building units (SBUs) within MOFs which inhibits further catalytic turnover. Herein, we developed a simple soaking procedure with a basic aqueous solution that reactivates the active sites of spent MOFs after organophosphate catalysis. Moreover, we develop amine functionalized MOF-808 derivatives through *de novo* synthesis with H_3-BTC-NH_2 (BTC = 1,3,5-benzenetricarboxylic acid) and post-synthetic modification (PSM) that are highly active for organophosphate hydrolysis under non-buffered aqueous conditions.

Nerve agents are chemical warfare agents (CWAs) that contain phosphate ester groups and are extremely toxic to the nervous system.[1] Organophosphonate compounds covalently bind to acetylcholinesterase (AChE) which is responsible for the catalytic breakdown of acetylcholine which functions as a neurotransmitter to muscles and organs.[2] Subsequent build-up of acetylcholine due to nerve agent poisoning prevents contraction of muscles and organs vital to respiration which may lead to asphyxiation or cardiac arrest.[3] Nerve agents can be rendered ineffective by enzymes through hydrolysis and cleavage of the P-X (X = F, CN or S) bond, however, enzyme catalysis is limited by their insufficient stability under practical conditions.[4] Consequently, robust materials capable of phosphate hydrolysis such as zeolites, polyoxometalates, metal oxides, and recently metal-organic frameworks (MOFs) have been explored for the destruction of CWAs.[5]

Metal-organic frameworks are porous materials comprised of organic struts which link to metal clusters, *i.e.* secondary building units (SBUs) forming hybrid ordered crystalline networks.[6] Utilization of Zr_6-based SBUs have resulted in chemically robust MOFs amenable to functionalization on the node and strut enabling their use in realistic conditions.[7,8,9,10] The Zr_6 SBU is ideally 12-connected, *i.e.* 12 carboxylic acids bound to the SBU, but 10, 8, 6 or 4-connectivity can be obtained depending on reaction conditions and the multi-topic organic strut employed in MOF synthesis.[11] MOFs containing SBUs less than 12 connectivity possess so-called "missing-linker" sites that are often initially occupied by mono carboxylic acid modulators.[12] Due to the chemical robustness of the Zr_6 SBU, many modulators can be readily removed through thermal or acidic activating conditions to give $Zr(OH)(OH_2)$ without significant structural damage to the framework.[13,14,15] These deficient linker sites have been utilized as active sites for catalysis.[16,17,18]

We and others have recently shown that these deficient "missing-linker" sites facilitate rapid organophosphate hydrolysis.[19,20] However, alkaline buffer conditions are often required for fast organophosphate hydrolysis rates.[21,22] Under solely aqueous conditions many Zr-MOFs facilitate slower hydrolysis.[23,24,25] In order to utilize these materials in protective gear for the warfighter, they must facilitate hydrolysis without volatile and caustic components. While solid-state amine buffered composites have been developed, they often lead to slower hydrolysis rates due to the inhomogeneity of the MOF filler particles with polymeric matrix components resulting in clustering of MOFs.[26] In addition, amine components are often needed in excess due to leaching from the composite.[27] Moreover, while many have labeled the hydrolysis of organophosphate with MOFs as catalytic, under solely aqueous conditions reaction sites are often poisoned due to phosphoric acid byproducts limiting subsequent catalytic turnover.[28] Consequently, buffer-like conditions must be integrated within MOFs themselves to enable fast and regenerative nerve agent catalytic hydrolysis in order for realistic use.

Herein, we demonstrate that the active site poisoning of spent Zr- or Hf-MOF catalysts can be remedied through

basic solutions which restores catalytic activity (Scheme 1). Furthermore we developed amine functionalized MOF-808 analogs through post-synthetic modification and *de novo* synthesis that outperform their non-functionalized counterparts as catalysts for organophosphate degradation under solely aqueous conditions (Scheme 2).

Scheme 1. SBU DMP poisoning and reactivation

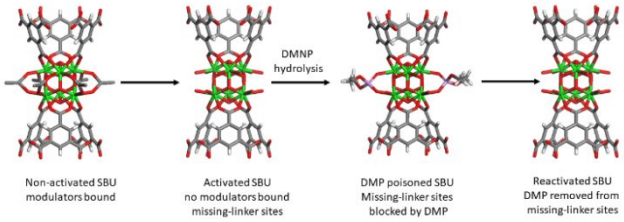

MOF catalytic poisoning and reactivation

Recently, we developed single-component MOFs that facilitated organophosphate hydrolysis under non-buffered conditions.[29] However, these first-generation catalysts proved to be limited upon repeated use. Mono-carboxylate modulators and solvent-assisted linker incorporated (SALI) moieties enabled higher initial pH values relative to their non-functionalized MOFs which facilitates faster initial dimethyl 4-nitrophenyl phosphate (DMNP) hydrolysis (Table 1 entries 5, 9). Unfortunately, the SBU active sites of these MOFs such as MOF-808-SALI-BA-Morph (BA=4-(morpholinomethyl)benzoic acid) become poisoned through byproducts (Figure 1). Hydrolysis causes a decrease in pH (~2) and modulator moieties are ultimately removed from the SBU and replaced with highly acidic dimethyl phosphate (DMP) as seen by ^{1}H NMR (Figures S10 and S11). Consequently, we set out to develop a washing procedure that restores catalytic activity to spent MOF catalysts. Given the inherent dangers of residual CWAs within spent MOFs, we focused on the utilization of CWA simulant DMNP which has been shown to mimic the reactivity of G-agents.[22]

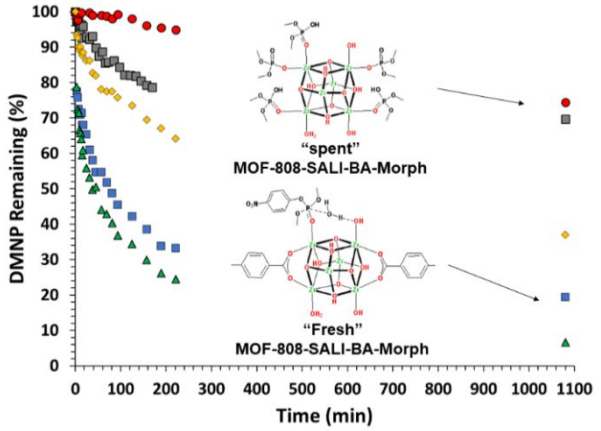

Figure 1. DMNP hydrolysis profiles of fresh Zr-MOF-808-SALI-BA-Morph (blue squares), spent Zr-MOF-808-SALI-BA-Morph (gray squares), fresh Hf-MOF-808-SALI-BA-Morph (green triangles), spent Hf-MOF-808-SALI-BA-Morph (red circles), spent Hf-MOF-808-SALI-BA-Morph treated with piperidine (yellow diamonds). DMNP (%) remaining as a function of time.

Recently, phosphate functionalized moieties were incorporated into zirconium based MOFs through SALI.[30] Unlike their carboxylate analogues, the phosphate groups are retained on the SBUs under acidic conditions. Conversely, the phosphate groups could be displaced under basic conditions such dimethylformamide (DMF) solutions of piperidine. Given that DMP is similar to phosphates, we sought to utilize piperidine as a means to dissociate it from the SBUs of spent MOF catalysts and restore organophosphate hydrolysis. While DMF is a common utilized solvent for MOF synthesis, its use under acidic conditions leads to decomposition into formic acid and dimethylammonium.[31] Moreover, Zr-MOFs are commonly unstable under basic environments.[32] Consequently, we sought to test the stability of Zr-MOF-808 under basic aqueous solutions of piperidine. As expected, concentrated aqueous solutions of piperidine at or above 0.1 M concentrations diminished MOF stability as observed through PXRD (Figures S1 and S2). However, MOF-808 proved to be stable to dilute aqueous piperidine solutions (13mM). In order to ascertain if piperidine would dissociate DMP from the SBUs of MOF-808, we functionalized MOF-808 with DMP through SALI. Careful utilization of DMP equivalents to MOF-808 (2:1) generated a crystalline material, (Figure S3) MOF-808-DMP, with two DMP moieties per SBU according to ^{1}H NMR of the digested MOF (Figures S4 and S5). Treatment of MOF-808-DMP with a piperidine solution at room temperature and subsequent washing with water and acetone generated MOF-808 with no detectable traces of DMP as evidenced by ^{1}H NMR (Figures S6 and S7). We then sought to test whether we could restore activity to poisoned MOF organophosphate hydrolysis catalysts with this procedure.

The main driving force for catalytic poisoning in a MOF catalyst is the strong affinity of byproducts to the metal centers of the SBU (Scheme 1). Consequently, we explored the effect of metal centers to both SALI dissociation and active site poisoning by utilizing Hf-MOFs as they are more oxophillic than their zirconium analogs. Hf-MOF-808-PA (PA = propanoic acid) and SALI amine functionalized analogs were derived from previous methods for Zr-MOF-808-PA synthesis, activation and modification (see Figures S8-S14, S23-38 for characterization).[29] Under exact catalytic aqueous conditions the various amine-SALI-functionalized Hf-MOF-808 catalysts significantly outperformed their zirconium analogs in the initial hydrolysis of DMNP (see Table 1 entries 9 & 10, Figures S87 and S92). Presumably, the enhanced activity is the consequence of better DMNP affinity to the missing-linker sites of Hf-MOF-808 relative to the Zr-MOF-808 sites. Indeed Islamoglu *et al*., recently demonstrated that Hf-NU-808 displayed enhanced water affinity relative to Zr-MOF-808 which was attributed to greater electronegativity of the Hf-SBU.[33] Conversely, Hf-MOFs should experience relatively more DMP active site poisoning than their zirconium analogs. Indeed, DMNP hydrolysis is more inhibited with spent Hf-MOF-808-SALI-BA-Morph than with Zr-MOF-808-SALI-BA-Morph upon repeated use (Figure 1).

In an attempt to restore catalytic activity, the spent Hf-MOF-808-SALI-BA-Morph was treated with aqueous

Scheme 2. Synthetic scheme for Zr-MOF-808-NH_2.

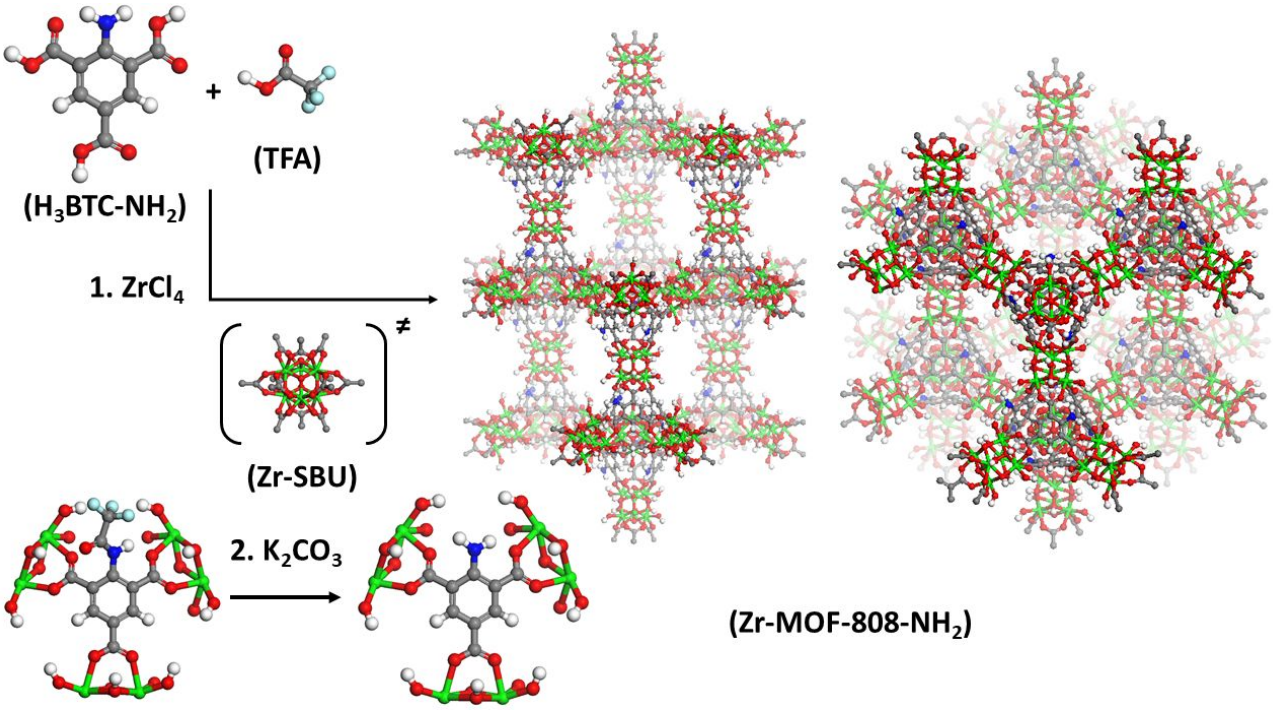

piperidine. As expected, the reactivated MOF displays a significant increase in DMNP hydrolysis (Figure 1). However, it must be highlighted that piperidine treatment displaced a significant amount of BA-Morph modulators (Figure S30). This contributed to lower than expected half-life of piperidine treated MOF relative to the fresh Hf-MOF-808-SALI-BA-Morph ($t_{1/2}$ = >220 min vs. 14 min, respectively). The displacement of SALI incorporated moieties by both organophosphate hydrolysis and piperidine treatment, forced us to utilize the organic struts of benzene-1,3,5- tricarboxylic acid (BTC) for the incorporation of amine co-catalyst into the MOF. Consequently, *de novo* MOF synthesis was attempted with H_3-BTC-NH_2 to generate amine functionalized MOF-808 analogs.

Synthesis of MOF-808-NH_2 and SBU activation

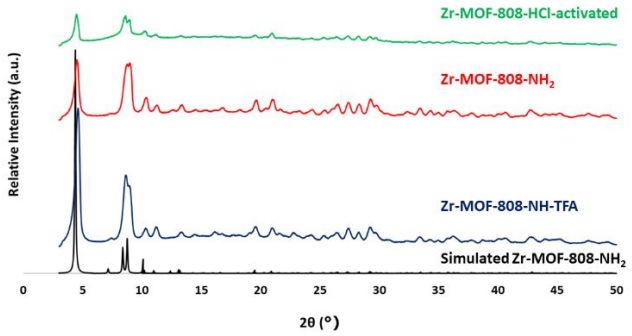

Figure 2. PXRD patterns of simulated Zr-MOF-808-NH-TFA (black), Zr-MOF-808-NH-TFA (blue), K_2CO_3-activated Zr-MOF-808-NH_2 (red), and HCl-activated Zr-MOF-808 (green).

To our knowledge there have been no reported synthesis of Zr- or Hf-MOF-808 derivatives with H_3-BTC-NH_2. Different synthetic conditions such as varying temperature and modulators failed to produce crystalline MOFs except in the instance with trifluoroacetic acid (TFA) as a modulator. After 5 days at 120 °C, the amine-functionalized linker generated microcrystalline powders (Figure 2) that had similar adsorption properties as the Zr-MOF-808-TFA analog (Table 1, entries 4, 15). Unfortunately, HCl treatment did not appear to facilitate full removal of TFA as evidenced by a lack of change in N_2 adsorption or pore-size distribution (Figures 4, S63). True removal of the TFA modulators should have caused a significant increase in N_2 uptake as a consequence of mass loss. In addition, TFA is still detected in the ^{19}F NMR spectrum after HCl treatment (Figure S64). A significant amount of IR stretches associated with TFA at 1240 cm^{-1} are still observable after HCl treatment (Figure S111). Moreover, removal of the TFA would greatly affect DMNP hydrolysis compared to the as synthesized amine-functionalized MOF-808. Surprisingly, DMNP hydrolysis with the HCl-treated Zr-MOF catalyst proved to be similar if not slightly slower than as synthesized amine-functionalized MOF precursor (Table 1, entries 15, 16). Consequently, alternative SBU activating conditions were attempted.

There are several reported post-synthetic methods for removal of SBU-bound modulators that vary from thermal

to acidic workup.[34] Unfortunately, these methods often complicate missing-linker activation. For instance, we recently demonstrated that HCl activation of Zr-MOF-808 in DMF concurrently removes modulators yet generates SBU bound formic acid (FA) and dimethylammonium chloride as a consequence of acidic DMF degradation.[29] Similarly,

Table 1. MOF surface area, pore size, DMNP half-life, SBU bound modulators before & after reaction, initial pH

(Entry #)/MOF	Surface area[a] (m^2g^{-1})	Pore size (Å)	t ½, DMP yield after 18 h[b]	Modultor before/after reaction[c]	Initial pH[d]
(1)Zr-MOF-808-PA	804	14.8	157 min, 89%	6/3	4
(2)Hf-MOF-808-PA	751	14.8	157 min, 86%	6/3	4
(3)Zr-MOF-808-AA	479	15.9	189 min, 78%	6/1	3
(4)Zr-MOF-808-TFA	1072	14.8	>221 min, 70%	-	2
(5)Zr-MOF-808-DMF-HCl- act	1734	15.9	>220 min, 71%	1/-	
(6)Zr-MOF-808-acetone-HCl-act	804	15.9	>220 min, 70%	1/-	2
(7)Hf-MOF-808-DMF-HCl-act	913	15.9	>220 min, 62%	3/-	
(8)Hf-MOF-808-acetone-HCl-act	1214	15.9	>220 min, 30%	1/-	2
(9)Zr-MOF-808-SALI-[BA-morph]$_2$	303	11.8	69 min, 80%	2/1	5
(10)Hf-MOF-808-SALI-[BA-morph]$_3$	476	14.8	14 min, 100%	3/1.5	5
(11)Zr-MOF-808-SALI-[BA-CH_2NH_2]$_3$[BA-CH_2-NH_3^+]$_1$	570	12.6	157 min, 82%	4/2.5	5
(12)Hf-MOF-808-SALI-[BA-CH_2NH_2]$_2$[BA-CH_2-NH_3^+]$_2$	740	13.6	59 min, 100%	4/2.5	4
(13)Zr-MOF-808-SALI-[BA-AO]$_2$	460	14.8	221 min, 87%	2/1	4
(14)Hf-MOF-808-SALI-[BA-AO]$_3$	618	12.7	69 min, 100%	3/2	4
(15)Zr-MOF-808-NH-TFA	1098	15.9	189 min, 80%	-	3
(16)Zr-MOF-808-NH-TFA-acetone-HCl-act	1067	15.9	>220 min, 80%	-	2
(17)Zr-MOF-808-NH_2-K_2CO_3-act	1450	18.6	57 min, 95%	-	5-6
(18)Zr-MOF-808-NH-Morph	1260	18.4	24 min, 100%	-	5
(19)Hf-MOF-808-NH-TFA	694	14.8	157 min, 85%	-	
(20)Hf-MOF-808-NH_2-K_2CO_3-act	894	15.9	69 min, 78%	-	5-6

PERFORMED UNDER NON-BUFFERED CONDITIONS WITH 12 MOL% MOF CATALYST LOADING. [A]BET SURFACE AREA. [B]DMP YIELD.[C]BASED ON ^{1}H NMR OF DIGESTED MOF.[D]PH OF 1 ML SOLUTION WITH MOF BEFORE DMNP ADDITION. SALI = SOLVENT ASSISTED LINKER INCORPORATION, PA = PROPANOIC ACID, AA = ACETIC ACID, TFA = TRIFLUOROACETIC ACID, BA-MORPH = 4-(MORPHOLINOMETHYL)BENZOIC ACID, BA-CH_2NH_2 = 4-(AMINOMETHYL)BENZOIC ACID, BA-AO = 4-(N′-HYDROXYCARBAMIMIDOYL)BENZOIC ACID, NH-MORPH = MOF-808-NH2 MODIFIED WITH 4-(2-CHLOROETHYL)MORPHOLINE, ACT = ACTIVATED, - = NOT AVAILABLE

Lu *et al.*, recently demonstrated that HCl activation in DMF also generates bound formic acid and dimethylammonium chloride within NU-1000.[35] Substitution of DMF with acetone during HCl activation could effectively remove SBU bound modulators without side product generation.[36] Indeed acetone-HCl activation of Hf-MOF-808-PA results in only < 1 PA per SBU while DMF-HCl activation generates <1 PA and 2 FA per SBU (Figures S25 and S14, respectively). Surprisingly, under aqueous conditions the DMF-HCl activated MOF facilitates faster DMNP conversion than acetone-HCl activation, presumably due to the higher amount SBU bound formic acid modulators and dimethylammonium chloride of the later. As mentioned earlier, some modulators can slightly increase the initial pH of solution consequently enhancing DMNP conversion. Another possibility that might address the interference with DMNP hydrolysis is steric hindrance as a consequence of amine reactivity of H_3-BTC-NH_2 with TFA during MOF formation.

While amine functionalized linkers have been utilized in MOF synthesis, their use in Zr-based MOF construction have often been problematic due to partial amine reactivity during MOF formation. Indeed, the first reported synthesis of Zr-UiO-66-NH_2 by Garibay *et al.*, in 2010 demonstrated that there were two distinct sets of aromatic peaks in the ^{1}H NMR spectrum of the digested MOF that

correspond to 2-aminoterephthalic acid and an unknown linker.[37] Subsequent studies by Zwolinski *et al.*, indicated that these mysterious peaks could be attributed to the formylation of the amine linker facilitated by DMF decomposition during MOF formation.[38] Recently, TFA modulators within the SBUs of Zr-MOF-808-TFA were successfully removed with aqueous HCl.[39] Given that HCl activation of Zr-MOF-808-NH_2-TFA retains TFA suggests that H_3-BTC-NH_2 may have reacted with TFA. Indeed, the TGA of the MOF contains three significant mass losses above 300 °C indicating that it is not solely comprised of Zr bound TFA, but also of H3BTC-NH_2 moieties (Figure S72).

In order to test whether the amines had reacted with TFA, we utilized a qualitative pseudo Schiff-base amine test with acetone. If the amine group were truly free within the MOF it would readily react with acetone to generate a Schiff base.[40] The qualitative Schiff-base amine test yielded no indication of free amines after exposure to acetone (Figure S104). Consequently, we sought to fully activate the amide moiety within MOF-808-NH-TFA through alternative procedures.

Acetyl amide deprotection is commonly facilitated through basic conditions.[41,42] Given the inherent instability of Zr-based MOFs towards basic conditions, we utilized a hot aqueous K_2CO_3 solution with Zr-MOF-808-NH-TFA that facilitated a white microcrystalline MOF with analogous PXRD pattern (Figure 2). As expected, K_2CO_3 activation of previously DMF-HCl treated Zr-MOF-808-NH-TFA facilitated enhanced N_2 adsorption of the MOF (Figure S63). Moreover, the TGA of K_2CO_3 treated MOF-808 indicates a significant decrease in Zr-bound and linker bound TFA (Figure S72). Another indication the basic activation worked is evident by ^{19}F NMR as TFA was not detected (Figure S64). As expected, the K_2CO_3 treated MOF underwent a significant color change from white to bright yellow upon acetone exposure, suggesting that basic activation afforded truly free amines within Zr-MOF-808-NH_2 (Figure S104). Infrared and ^1H NMR spectroscopy corroborate amine formation (Figure S109). Hf-MOF-808-NH-TFA appears to be more unstable toward basic conditions than its Zr analog which necessitates basic activation with one-half K_2CO_3 concentration. With our optimized MOF activation technique in hand we sought to benchmark the efficacy of Zr- and Hf-MOF-808-NH_2 materials in organophosphate hydrolysis through the degradation of a nerve agent simulant DMNP.

DMNP hydrolysis with MOF-808-NH_2 materials

Recently, Islamoglu *et al.*, utilized various amine functionalized linkers to construct amine functionalized NU-1000 analogs and explored the effects of amines on DMNP hydrolysis under buffered conditions.[43] These studies demonstrated that the position of the amine on the carboxylate aromatic ring (*ortho* vs. *meta*) of the strut had a profound impact on DMNP hydrolysis. The authors attribute the higher activity of the *ortho* functionalized MOF to the proximal location of the amine to missing linker sites and enhanced hydrogen bonding interactions towards the DMNP substrate. Given that there are two BTC-NH_2 linkers per SBU, the amine groups should be proximal to two missing-linker active sites which should enhance DMNP hydrolysis relative to MOF-808. As expected, Zr-MOF-808-NH_2 significantly outperformed HCl-activated Zr-MOF-808 in the hydrolysis of DMNP under solely aqueous conditions with $t_{1/2}$ = 57 and 220 min, respectively (Figures 3, S84). As stated previously, due to relatively higher metal oxophilicity Hf-MOFs are significantly faster in DMNP hydrolysis yet succumb more readily to catalytic poisoning than their zirconium analogs. This DMNP hydrolysis trend is also evident with the MOF-808-NH_2 system. The initial DMNP hydrolysis rate with Hf-MOF-808-NH_2 is nearly three times faster than the initial DMNP hydrolysis rate with Zr-MOF-808-NH_2 (Figure S106). Nonetheless, Zr-MOF-808-NH_2 has higher conversion after 18 hours than its hafnium analog (95% vs 78% conversion). While amine functionality may significantly contribute to enhanced hydrolysis, we wanted to rule any discrepancies with differing SBU activation conditions.

Many groups have recently shown that the missing-linker sites within Zr_6-SBUs offer tethering site for hetero metal coordinative incorporation.[44] Since cationic potassium is generated during basic activation whether it incorporated into the SBUs of MOF-808-NH_2 was explored. Through SEM-EDS analysis trace amounts of potassium were observed (40:1 Zr:K), however, they were primarily situated in the exterior of the MOF particle (Figure S105). In order to truly correlate enhanced activity with the amines, hydrolysis was tested with K_2CO_3 activated non-linker functionalized Zr-MOF-808-PA. Similar to acetone-HCl activation, K_2CO_3 activation of MOF-808-PA removed 5 out of 6 PA modulatros and produced a SBU environment of $Zr_6O_4(OH)_4(BTC)_2(PA)_1(OH_2)_5(OH)_5$ as indicated by ^1H NMR of the digested MOFs sample (Figure S107). Not surprisingly, K_2CO_3 activated Zr-MOF-808-PA displays similar DMNP hydrolysis to acetone-HCl activated Zr-MOF-808, however, they are both magnitudes slower than K_2CO_3 activated Zr-MOF-808-NH_2 (t ½ = >220 min vs. 57 min) (Figures S108, S84, S98). Likewise, the K_2CO_3 activated Hf-MOF-808-NH_2 significantly outperformed the acetone-HCl activated Hf-MOF-808 with 78% vs. 30% conversion after 18 h (Figures S101, S86).

While the differences in DMNP hydrolysis activity between MOF-808 and MOF-808-NH_2 might suggest that the amine-functionality is enhancing hydrolysis, it must be stated that it alone is not the sole factor. Basic SBU activation with K_2CO_3 generates relatively more accessible active sites compared to HCl activation. Given the ability of activated SBUs to bind to Cl, HCl activation may interfere with DMNP binding and hydrolysis. A more rational explanation for the observed differences in activity are the highly contrasting initial pH differences among K_2CO_3 activated Zr-, Hf-MOF-808-NH_2 and non-functionalized HCl activated Zr-, Hf-MOF-808 (Table 1,

entries 16-18, 20) under catalytic conditions (12 mol% MOF loading, 1 mL H_2O).

While better activated SBUs might facilitate enhanced DMNP hydrolysis, it must be highlighted that alteration of the synthetic conditions, such as modulator or scale, have a pronounced effect on particle size which results in changes in catalysis. When Zr-MOF-808-PA is synthesized under scaled up conditions (5x, 72 h), it alters the particle size distribution (Figure 103), and behaves differently than a small scale version in the hydrolysis of DMNP due to particle agglomeration (Figures S79, S108). To summarize, the amine functionality within Zr- or Hf-MOF-808-NH_2 is not the sole factor for the dramatic enhancement of DMNP relative to their non-functionalized analogs, however, it appears to have a significant contribution.

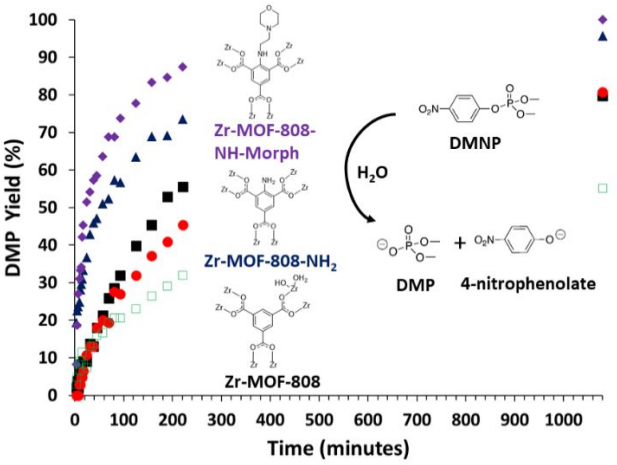

Figure 3. DMNP hydrolysis profile of as synthesized Zr-MOF-808-NH-TFA (black squares), after HCl-activation (red circles), after K_2CO_3-activation (blue triangles), Zr-MOF-808-NH-Morph (purple diamonds), and Zr-MOF-808-PA(5x) after K_2CO_3-activation (green unfilled squares) under solely aqueous conditions at 12% mol MOF catalyst loading.

Post-synthetic modification of Zr-MOF-808-NH_2

As previously demonstrated from our SALI-functionalized Zr-MOFs studies, amine co-catalysts with higher basicities such as morpholino groups tend to enhance organophosphate hydrolysis under non-buffered conditions.[29] We sought to further enhance organophosphate hydrolysis through the tethering of morpholino groups through haloalkylation with 4-(2-chloroethyl)morpholine (Scheme 3), given that the aromatic amines within MOFs tend to readily undergo reactivity through postsynthetic modification (PSM).[10, 45] Modification of Zr-MOF-808-NH_2 with the morpholino group did not significantly affect crystallinity as confirmed by PXRD (Figure S69), however, a slight decrease in N_2 adsorption and pore size was observed (Figures 4, S63, S68). The IR spectra contains new stretches associated with alkane C-H (2900-2800 cm-1), and ether C-O (1029 cm-1) groups (Figure S111). The ^{1}H NMR of the digested modified MOF contains new peaks and does not contain any peaks associated with BTC-NH_2 of the parent MOF suggesting full modification (Figure S70).

Scheme 3. Synthetic scheme for Zr-MOF-808-NH-Morph through post-synthetic modification.

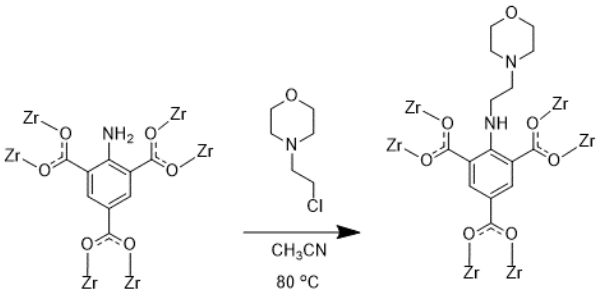

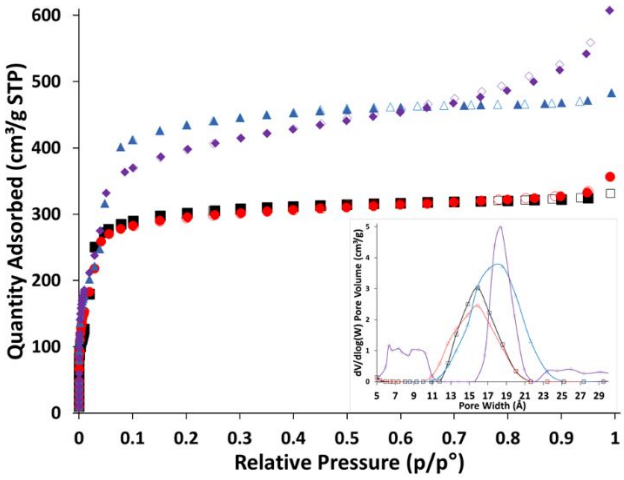

Figure 4. $N_{2\ (g)}$ adsorption isotherms of Zr-MOF-808-NH-TFA (black squares), Zr-MOF-808-NH-TFA after HCl activation (red circles), Zr-MOF-808-NH-TFA after K2CO3 activation (blue triangles), and Zr-MOF-808-NH-Morph (purple diamonds). Filled symbols = adsorption, Unfilled = desorption. Inset graph illustrates pore size distribution of the corresponding MOFs.

With morpholino groups attached to adjacent missing-linker SBU active sites we explored their effect on reactivity in DMNP hydrolysis. The morpholino-functionalized MOF, Zr-MOF-808-NH-Morph, significantly outperformed the parent Zr-MOF-808-NH_2 (t ½ = 24 min vs. 57 min (Figure 3). Unfortunately, similar to other Zr-based MOFs, MOF-808-NH_2 analogs suffer from catalytic poisoning after hydrolysis (Figure 5). However, it must be noted that the reuse of spent Zr-MOF-808-NH-Morph significantly outperformed non-linker SALI functionalized MOF Zr-MOF-808-SALI-BA-Morph in the hydrolysis of fresh DMNP (50% vs 30% conversion after 18h) (Figure S110). The reduction in active site poisoning may be a consequence of the tethered morpholino species inhibiting DMP binding to the SBU.

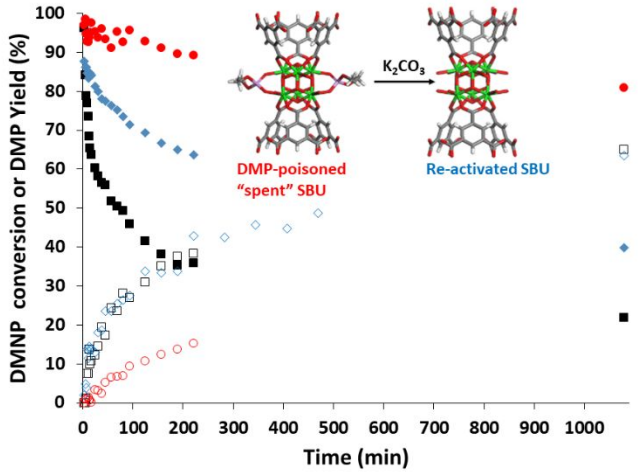

Figure 5. DMNP conversion with Hf-MOF-808-NH_2 (filled) and DMP Yield with Zr-MOF-808-PA-5x (unfilled) catalysts initially (black squares), reused (red circles), and reactivated (blue diamonds) under solely aqueous conditions.

Reactivation of spent MOF-808-NH_2 systems

Given that basic conditions with piperidine and K_2CO_3 are effective for the removal of DMP and TFA modulators, we attempted to reactivate spent and poisoned MOFs. Unfortunately, treatment of aqueous piperidine did not successfully restore hydrolytic stability to spent Zr-MOF-808-NH-Morph. While piperidine was shown to successfully remove DMP from the SBU of SALI functionalized Zr-MOF-808-DMP, it may not be applicable to spent catalytic MOFs that utilized excess DMNP/DMP (2 DMP per SBU vs. 8.8x molar excess). Consequently, we repurposed our newly derived MOF K_2CO_3 activation procedure in an attempt to reactivate spent MOFs. Given that hafnium MOF systems display relatively more DMP poisoning than their zirconium analogs, we initially focused on the reactivation of spent Hf-MOF-808-NH_2. The supernatant containing DMP in the NMR tube was removed from the spent Hf-MOF-808-NH_2 which was subsequently treated with hot aqueous K_2CO_3 under static conditions for 18 h and solvent exchanged multiple times with fresh water. As seen in Figure 5, basic treatment restored a significant amount of hydrolysis, however, it did not fully restore the fast activity of the first run observed with Hf-MOF-808-NH_2. We speculate that a significant amount of MOF sample was lost during the multiple solvent exchanges within the NMR tube. Consequently, we utilized spent Zr-MOF-808-PA-5x because the agglomerated particles lessened the possibility of mass loss during solvent exchange during the re-activation procedure. As expected, treatment with K_2CO_3 fully restored the initial activity of Zr-MOF-808-PA-5x (Figure 5).

Conclusion

We have shown that loss of activity due to the poisoning of Zr or Hf missing-linker sites within MOF organophosphate hydrolysis catalysts can be restored through dilute basic aqueous conditions. Given that solvent-assisted linker incorporated (SALI) amine co-catalysts dissociate after organophosphate hydrolysis, we utilized post-synthetic modification (PSM) to covalently tether amine co-catalyst to the organic strut adjacent to the missing-linker sites of SBUs catalysts. To our knowledge, this report contains the first synthesis of Zr- and Hf-MOF-808-NH_2 derived through *de novo* MOF synthesis with BTC-NH_2. As a consequence of amine reactivity with TFA modulators during MOF formation, we developed an aqueous deprotection procedure with K_2CO_3 that additionally removes TFA modulators and poisoning organophosphate hydrolysis byproducts from the SBU. The basic activation procedure that facilitates efficient missing-linker generation along with an increase in pH, and the amine functionality of BTC-NH_2 are factors in the significant enhancement of DMNP hydrolysis with Zr-MOF-808-NH_2 relative to HCl-activated Zr-MOF-808 under solely aqueous conditions. Post-synthetic modification of Zr-MOF-808-NH_2 with 4-(2-chloroethyl)morpholine generated Zr-MOF-808-NH-Morph which is more active in DMNP hydrolysis than the native MOF-808 catalyst in aqueous non-buffered conditions. These newly synthesized, highly active catalysts, along with our regenerative basic post-treatment activation technique, are critical advancements for the practical and recyclable utilization of MOFs as organophosphate hydrolysis catalyst within fibers or composites for nerve agent protection.

ASSOCIATED CONTENT

Supporting Information.

Synthetic procedures of MOF materials, PXRD patterns, SEM data, N_2 sorption isotherms, ^1H and ^{31}P NMR spectra, TGA, methods of hydrolysis. This material is available free of charge via the Internet at http://pubs.acs.org.

AUTHOR INFORMATION

Corresponding Author

* Jared B. Decoste, jared.b.decoste2.civ@army.mil

Author Contributions

S.J.G. wrote the original draft input from all authors. All authors were involved in reviewing and editing the manuscript. The manuscript was conceptualized by S.J.G., G.W.P., and J.B.D. Investigation was conducted by S.J.G., and T.M.T., with formal analysis conducted by I.O.I.

Notes

The authors declare no competing financial interests.

ACKNOWLEDGMENT

This work was supported by Defense Threat Reduction Agency the Joint Science and Technology Office for Chemical and Biological Defense (JSTO–CBD).

REFERENCES

(1) Hilmas, C.; Smart, J.; Hill, B. Medical aspects of chemical warfare. *Tuorinsky. SD ed* **2008**.

(2) Mercey, G.; Verdelet, T.; Renou, J.; Kliachyna, M.; Baati, R.; Nachon, F.; Jean, L.; Renard, P.-Y. Reactivators of acetylcholinesterase inhibited by organophosphorus nerve agents. *Accounts of chemical research* **2012**, *45* (5), 756-766.

(3) Colović, M. B.; Krstić, D. Z.; Lazarević-Pašti, T. D.; Bondžić, A. M.; Vasić, V. M. Acetylcholinesterase inhibitors: pharmacology and toxicology. *Curr Neuropharmacol* **2013**, *11* (3), 315-335. DOI: 10.2174/1570159x11311030006 From NLM.

(4) Li, P.; Chen, Q.; Wang, T. C.; Vermeulen, N. A.; Mehdi, B. L.; Dohnalkoya, A.; Browning, N. D.; Shen, D.; Anderson, R.; Gomez-Gualdron, D. A.; et al. Hierarchically Engineered Mesoporous Metal-Organic Frameworks toward Cell-free Immobilized Enzyme Systems. *Chem* **2018**, *4* (5), 1022-1034. DOI: 10.1016/j.chempr.2018.03.001.

(5) Smith, B. M. Catalytic methods for the destruction of chemical warfare agents under ambient conditions. *Chemical Society Reviews* **2008**, *37* (3), 470-478. DOI: 10.1039/b705025a.

(6) Kalmutzki, M. J.; Hanikel, N.; Yaghi, O. M. Secondary building units as the turning point in the development of the reticular chemistry of MOFs. *Science Advances* **2018**, *4* (10). DOI: 10.1126/sciadv.aat9180.

(7) Bai, Y.; Dou, Y. B.; Xie, L. H.; Rutledge, W.; Li, J. R.; Zhou, H. C. Zr-based metal-organic frameworks: design, synthesis, structure, and applications. *Chemical Society Reviews* **2016**, *45* (8), 2327-2367. DOI: 10.1039/c5cs00837a.

(8) Ha, J.; Lee, J. H.; Moon, H. R. Alterations to secondary building units of metal-organic frameworks for the development of new functions. *Inorganic Chemistry Frontiers* **2020**, *7* (1), 12-27. DOI: 10.1039/c9qi01119f.

(9) Kim, M.; Cohen, S. M. Discovery, development, and functionalization of Zr(IV)-based metal-organic frameworks. *Crystengcomm* **2012**, *14* (12), 4096-4104. DOI: 10.1039/c2ce06491j.

(10) Kalaj, M.; Cohen, S. M. Postsynthetic Modification: An Enabling Technology for the Advancement of Metal-Organic Frameworks. *Acs Central Science* **2020**, *6* (7), 1046-1057. DOI: 10.1021/acscentsci.0c00690.

(11) Chen, Z.; Hanna, S. L.; Redfern, L. R.; Alezi, D.; Islamoglu, T.; Farha, O. K. Reticular chemistry in the rational synthesis of functional zirconium cluster-based MOFs. *Coordination Chemistry Reviews* **2019**, *386*, 32-49. DOI: 10.1016/j.ccr.2019.01.017.

(12) Schaate, A.; Roy, P.; Godt, A.; Lippke, J.; Waltz, F.; Wiebcke, M.; Behrens, P. Modulated Synthesis of Zr-Based Metal-Organic Frameworks: From Nano to Single Crystals. *Chemistry-a European Journal* **2011**, *17* (24), 6643-6651. DOI: 10.1002/chem.201003211.

(13) Shearer, G. C.; Chavan, S.; Bordiga, S.; Svelle, S.; Olsbye, U.; Lillerud, K. P. Defect Engineering: Tuning the Porosity and Composition of the Metal-Organic Framework UiO-66 via Modulated Synthesis. *Chemistry of Materials* **2016**, *28* (11), 3749-3761. DOI: 10.1021/acs.chemmater.6b00602.

(14) Feng, D. W.; Gu, Z. Y.; Li, J. R.; Jiang, H. L.; Wei, Z. W.; Zhou, H. C. Zirconium-Metalloporphyrin PCN-222: Mesoporous Metal-Organic Frameworks with Ultrahigh Stability as Biomimetic Catalysts. *Angewandte Chemie-International Edition* **2012**, *51* (41), 10307-10310. DOI: 10.1002/anie.201204475.

(15) Mondloch, J. E.; Bury, W.; Fairen-Jimenez, D.; Kwon, S.; DeMarco, E. J.; Weston, M. H.; Sarjeant, A. A.; Nguyen, S. T.; Stair, P. C.; Snurr, R. Q.; et al. Vapor-Phase Metalation by Atomic Layer Deposition in a Metal-Organic Framework. *Journal of the American Chemical Society* **2013**, *135* (28), 10294-10297. DOI: 10.1021/ja4050828.

(16) Taddei, M. When defects turn into virtues: The curious case of zirconium-based metal-organic frameworks. *Coordination Chemistry Reviews* **2017**, *343*, 1-24. DOI: 10.1016/j.ccr.2017.04.010.

(17) Feng, L.; Day, G. S.; Wang, K. Y.; Yuan, S.; Zhou, H. C. Strategies for Pore Engineering in Zirconium Metal-Organic Frameworks. *Chem* **2020**, *6* (11), 2902-2923. DOI: 10.1016/j.chempr.2020.09.010.

(18) Rimoldi, M.; Howarth, A. J.; DeStefano, M. R.; Lin, L.; Goswami, S.; Li, P.; Hupp, J. T.; Farha, O. K. Catalytic Zirconium/Hafnium-Based Metal-Organic Frameworks. *Acs Catalysis* **2017**, *7* (2), 997-1014. DOI: 10.1021/acscatal.6b02923.

(19) Peterson, G. W.; Destefano, M. R.; Garibay, S. J.; Ploskonka, A.; McEntee, M.; Hall, M.; Karwacki, C. J.; Hupp, J. T.; Farha, O. K. Optimizing Toxic Chemical Removal through Defect-Induced UiO-66-NH2 Metal-Organic Framework. *Chemistry-a European Journal* **2017**, *23* (63), 15913-15916. DOI: 10.1002/chem.201704525.

(20) Kirlikovali, K. O.; Chen, Z. J.; Islamoglu, T.; Hupp, J. T.; Farha, O. K. Zirconium-Based Metal-Organic Frameworks for the Catalytic Hydrolysis of Organophosphorus Nerve Agents. *Acs Applied Materials & Interfaces* **2020**, *12* (13), 14702-14720. DOI: 10.1021/acsami.9b20154.

(21) Katz, M. J.; Klet, R. C.; Moon, S. Y.; Mondloch, J. E.; Hupp, J. T.; Farha, O. K. One Step Backward Is Two Steps Forward: Enhancing the Hydrolysis Rate of UiO-66 by Decreasing OH-. *Acs Catalysis* **2015**, *5* (8), 4637-4642. DOI: 10.1021/acscatal.5b00785.

(22) Ploskonka, A. M.; DeCoste, J. B. Insight into organophosphate chemical warfare agent simulant hydrolysis in metal-organic frameworks. *Journal of Hazardous Materials* **2019**, *375*, 191-197. DOI: 10.1016/j.jhazmat.2019.04.044.

(23) Wang, H.; Mahle, J. J.; Tovar, T. M.; Peterson, G. W.; Hall, M. G.; DeCoste, J. B.; Buchanan, J. H.; Karwacki, C. J. Solid-Phase Detoxification of Chemical Warfare Agents using Zirconium-Based Metal Organic Frameworks and the Moisture Effects: Analyze via Digestion. *Acs Applied Materials & Interfaces* **2019**, *11* (23), 21109-21116. DOI: 10.1021/acsami.9b04927.

(24) de Koning, M. C.; Soares, C. V.; van Grol, M.; Bross, R. P. T.; Maurin, G. Effective Degradation of Novichok Nerve Agents by the Zirconium Metal-Organic Framework MOF-808. *Acs Applied Materials & Interfaces*. DOI: 10.1021/acsami.1c24295.

(25) de Koning, M. C.; van Grol, M.; Breijaert, T. Degradation of Paraoxon and the Chemical Warfare Agents VX, Tabun, and Soman by the Metal-Organic Frameworks UiO-66-NH2, MOF-808, NU-1000, and PCN-777. *Inorganic Chemistry* **2017**, *56* (19), 11804-11809. DOI: 10.1021/acs.inorgchem.7b01809.

(26) Lu, A. X.; McEntee, M.; Browe, M. A.; Hall, M. G.; DeCoste, J. B.; Peterson, G. W. MOFabric: Electrospun Nanofiber Mats from PVDF/UiO-66-NH2 for Chemical Protection and Decontamination. *Acs Applied Materials & Interfaces* **2017**, *9* (15), 13632-13636. DOI: 10.1021/acsami.7b01621.

(27) Dwyer, D. B.; Dugan, N.; Hoffman, N.; Cooke, D. J.; Hall, M. G.; Tovar, T. M.; Bernier, W. E.; DeCoste, J.; Pomerantz, N. L.; Jones, W. E. Chemical Protective Textiles of UiO-66-Integrated PVDF Composite Fibers with Rapid Heterogeneous Decontamination of Toxic Organophosphates. *Acs Applied Materials & Interfaces* **2018**, *10* (40), 34585-34591. DOI: 10.1021/acsami.8b11290.

(28) Liao, Y. J.; Sheridan, T.; Liu, J.; Farha, O.; Hupp, J. Product Inhibition and the Catalytic Destruction of a Nerve Agent Simulant by Zirconium-Based Metal-Organic Frameworks. *Acs Applied Materials & Interfaces* **2021**, *13* (26), 30565-30575. DOI: 10.1021/acsami.1c05062.

(29) Garibay, S. J.; Farha, O. K.; DeCoste, J. B. Single-component frameworks for heterogeneous catalytic hydrolysis of organophosphorous compounds in pure water. *Chemical Communications* **2019**, *55* (49), 7005-7008. DOI: 10.1039/c9cc02236h.

(30) Deria, P.; Bury, W.; Hod, I.; Kung, C. W.; Karagiaridi, O.; Hupp, J. T.; Farha, O. K. MOF Functionalization via Solvent-Assisted Ligand Incorporation: Phosphonates vs Carboxylates. *Inorganic Chemistry* **2015**, *54* (5), 2185-2192. DOI: 10.1021/ic502639v.

(31) Cottineau, T.; Richard-Plouet, M.; Mevellec, J. Y.; Brohan, L. Hydrolysis and Complexation of N,N-Dimethylformamide in New Nanostructurated Titanium Oxide Hybrid Organic-Inorganic Sols and Gel. *Journal of Physical Chemistry C* **2011**, *115* (25), 12269-12274. DOI: 10.1021/jp201864g.

(32) Buzek, D.; Demel, J.; Lang, K. Zirconium Metal-Organic Framework UiO-66: Stability in an Aqueous Environment and Its Relevance for Organophosphate Degradation. *Inorganic Chemistry* **2018**, *57* (22), 14290-14297. DOI: 10.1021/acs.inorgchem.8b02360. DeCoste, J. B.; Peterson, G. W.; Jasuja, H.; Glover, T. G.; Huang, Y. G.; Walton, K. S. Stability and degradation mechanisms of metal-organic frameworks containing the Zr6O4(OH)(4) secondary building unit. *Journal of Materials Chemistry A* **2013**, *1* (18), 5642-5650. DOI: 10.1039/c3ta10662d.

(33) Islamoglu, T.; Ray, D.; Li, P.; Majewski, M. B.; Akpinar, I.; Zhang, X.; Cramer, C. J.; Gagliardi, L.; Farha, O. K. From Transition Metals to Lanthanides to Actinides: Metal-Mediated Tuning of Electronic Properties of Isostructural Metal-Organic Frameworks. *Inorganic Chemistry* **2018**, *57* (21), 13246-13251. DOI: 10.1021/acs.inorgchem.8b01748.

(34) Vermoortele, F.; Bueken, B.; Le Bars, G.; Van de Voorde, B.; Vandichel, M.; Houthoofd, K.; Vimont, A.; Daturi, M.; Waroquier, M.; Van Speybroeck, V.; et al. Synthesis Modulation as a Tool To Increase the Catalytic Activity of Metal-Organic Frameworks: The Unique Case of UiO-66(Zr). *Journal of the American Chemical Society* **2013**, *135* (31), 11465-11468. DOI: 10.1021/ja405078u.

(35) Lu, Z. Y.; Liu, J.; Zhang, X.; Liao, Y. J.; Wang, R.; Zhang, K.; Lyu, J. F.; Farha, O. K.; Hupp, J. T. Node-Accessible Zirconium MOFs. *Journal of the American Chemical Society* **2020**, *142* (50), 21110-21121. DOI: 10.1021/jacs.0c09782.

(36) Kirlikovali, K. O.; Chen, Z. J.; Wang, X. J.; Mian, M. R.; Alayoglu, S.; Islamoglu, T.; Farha, O. K. Investigating the Influence of Hexanuclear Clusters in Isostructural Metal-Organic Frameworks on Toxic Gas Adsorption. *Acs Applied Materials & Interfaces* **2022**, *14* (2), 3048-3056. DOI: 10.1021/acsami.1c20518.

(37) Garibay, S. J.; Cohen, S. M. Isoreticular synthesis and modification of frameworks with the UiO-66 topology. *Chemical Communications* **2010**, *46* (41), 7700-7702. DOI: 10.1039/c0cc02990d.

(38) Zwolinski, K. M.; Nowak, P.; Chmielewski, M. J. Towards multifunctional MOFs - transforming a side reaction into a post-synthetic protection/deprotection method. *Chemical Communications* **2015**, *51* (49), 10030-10033. DOI: 10.1039/c5cc03469h.

(39) Liu, X. Y.; Kirlikovali, K. O.; Chen, Z. J.; Ma, K. K.; Idrees, K. B.; Cao, R.; Zhang, X.; Islamoglu, T.; Liu, Y. L.; Farha, O. K. Small Molecules, Big Effects: Tuning Adsorption and Catalytic Properties of Metal-Organic Frameworks. *Chemistry of Materials* **2021**, *33* (4), 1444-1454. DOI: 10.1021/acs.chemmater.0c04675.

(40) Li, Z.; Fang, M.; LaGasse, M. K.; Askim, J. R.; Suslick, K. S. Colorimetric Recognition of Aldehydes and Ketones. *Angewandte Chemie-International Edition* **2017**, *56* (33), 9860-9863. DOI: 10.1002/anie.201705264.

(41) El Kazzouli, S.; Koubachi, J.; Berteina-Raboin, S.; Mouaddib, A.; Guillaumet, G. A mild and selective method for the N-Boc deprotection by sodium carbonate. *Tetrahedron Letters* **2006**, *47* (48), 8575-8577. DOI: 10.1016/j.tetlet.2006.09.129.

(42) Tom, N. J.; Simon, W. M.; Frost, H. N.; Ewing, M. Deprotection of a primary Boc group under basic conditions. *Tetrahedron Letters* **2004**, *45* (5), 905-906. DOI: 10.1016/j.tetlet.2003.11.108.

(43) Islamoglu, T.; Ortuno, M. A.; Proussaloglou, E.; Howarth, A. J.; Vermeulen, N. A.; Atilgan, A.; Asiri, A. M.; Cramer, C. J.; Farha, O. K. Presence versus Proximity: The Role of Pendant Amines in the Catalytic Hydrolysis of a Nerve Agent Simulant. *Angewandte Chemie-International Edition* **2018**, *57* (7), 1949-1953. DOI: 10.1002/anie.201712645.

(44) Syed, Z. H.; Sha, F. R.; Zhang, X.; Kaphan, D. M.; Delferro, M.; Farha, O. K. Metal-Organic Framework Nodes as a Supporting Platform for Tailoring the Activity of Metal Catalysts. *Acs Catalysis* **2020**, *10* (19), 11556-11566. DOI: 10.1021/acscatal.0c03056.

(45) Cohen, S. M. The Postsynthetic Renaissance in Porous Solids. *Journal of the American Chemical Society* **2017**, *139* (8), 2855-2863. DOI: 10.1021/jacs.6b11259.